Remote sensing of vertical distributions of smoke aerosol off the coast of Africa

Y. J. Kaufman,[1] J. M. Haywood,[2] P. V. Hobbs,[3] W. Hart,[4] R. Kleidman,[4] and B. Schmid[5]

Received 5 February 2003; revised 3 June 2003; accepted 17 June 2003; published 16 August 2003.

[1] In 2004 NASA plans to launch the Cloud-Aerosol Lidar and Infrared Pathfinder Satellite Observations—CALIPSO mission, with a two-wavelength lidar aboard. CALIPSO will fly in formation with the Moderate Resolution Imaging Spectro-Radiometer (MODIS) on the Aqua satellite. Here we present inversions of combined aircraft lidar and MODIS data to study the properties of smoke off the southwest coast of Southern Africa. The inversion derives profiles of the aerosol extinction due to fine and coarse particles. Comparisons with three sets of airborne in situ measurements show excellent agreement of the aerosol extinction profiles; however the inversion derives smaller spectral dependence of the extinction than the in situ measurements. The inversion is sensitive to the aerosol backscattering-to-extinction ratio (BER). Due to nonsphericity of the coarse aerosols, the range of BERs of the smoke aerosol is 0.014 to 0.021 sr^{-1} for the fine and coarse particles at 0.53 and 1.06 μm wavelengths, which do not differ much from the value for dust (0.016 sr^{-1}) at these wavelengths. *INDEX TERMS:* 0305 Atmospheric Composition and Structure: Aerosols and particles (0345, 4801); 0933 Exploration Geophysics: Remote sensing; 1610 Global Change: Atmosphere (0315, 0325); 1640 Global Change: Remote sensing. **Citation:** Kaufman, Y. J., J. M. Haywood, P. V. Hobbs, W. Hart, R. Kleidman, and B. Schmid, Remote sensing of vertical distributions of smoke aerosol off the coast of Africa, *Geophys. Res. Lett.*, *30*(16), 1831, doi:10.1029/2003GL017068, 2003.

1. Introduction

[2] The CALIPSO spaceborne lidar will provide profiles of the attenuated backscattering coefficients of aerosols and clouds at wavelengths of 0.53 and 1.06 μm. It will fly in formation with the Aqua satellite with a MODIS instrument aboard. Over the oceans, analysis of the lidar data, combined with spectral measurements from MODIS, will combine vertical profile information from CALIPSO with detailed particle size information from MODIS. This should resolve most of the ambiguity in deriving aerosol profiles from the lidar measurements alone.

[3] Detailed profiles of aerosols and clouds, which distinguish fine and coarse particles, is needed to quantify the effects of aerosols on radiative forcing of climate, cloud structure, precipitation and the hydrological cycle [*Haywood and Boucher*, 2000; *Ramanathan et al.*, 2001; *Kaufman et al.*, 2002]. Measurements of the vertical distributions of smoke and pollution aerosols, which carry with them black carbon, are needed to study the effects of aerosol heating of the atmosphere, cooling the Earth's surface and modification to precipitation patterns [*Menon et al.*, 2002; *Lelieveld et al.*, 2002].

[4] We recently developed a technique that combines daytime MODIS and lidar data over the oceans [*Léon et al.*, 2003; *Kaufman et al.*, 2003] to resolve profiles of the extinction coefficient of fine and coarse particles. Here we apply this technique to data collected on Sept. 11, 2000 by MODIS and an airborne lidar off the west coast of Africa during the SAFARI 2000 field experiment [*Swap et al.*, 2002], and we compare the results with in situ airborne measurements. The main aerosol in the atmosphere was smoke advected from Africa [*Haywood et al.*, 2003].

2. Measurements

[5] The data presented in this paper were acquired on Sept. 11, 2000 in the vicinity of 22.5°S and 12.2°E. The lidar operated from the NASA ER-2 aircraft at 20 km altitude [*Spinhirne et al.*, 1989; *McGill et al.*, 2003] provided backscattering attenuated coefficients at wavelengths of 0.53 and 1.06 μm along the track of the aircraft. Results collected during the MODIS pass at 0945 UTC (Figure 1) are shown in Figure 2. The solar zenith angle during the MODIS pass of 34° and nadir view corresponds to glint angle of 34°, lower than the threshold of 40° in the MODIS operational aerosol algorithm. Both the high resolution data (altitude resolution of 15 m) and the averaged data (averaged over 0.3 km altitude intervals for aircraft altitude <7 km and over 0.9 km intervals for altitude >7 km) are shown. Both data sets were also averaged over 9 km distance along the aircraft track.

[6] In situ measurements of the aerosol scattering coefficient σ_{sca} (km^{-1}) were collected from two aircraft: the Met Office C-130, which performed two profiles at 0657 to 0718 UTC and at 1231 to 1305 UTC located not far from the lidar measurements (22.4°S, 12.7°E, and 22.9°S, 13.7°E respectively) [*Haywood et al.*, 2003] and the University of Washington's CV-580 [*Hobbs*, 2003] at 1030–1100 UTC and 23.1°S, 12.4°E. The spectral scattering coefficients were measured with nephelometers and corrected using the procedures described by *Anderson and Ogren* [1998]. Particle number concentrations were also measured aboard the C-130 and CV-580. The measurements are shown in

[1]NASA Goddard Space Flight Center, Laboratory for Atmospheres, Greenbelt, Maryland, USA.
[2]Met Office, Bracknell, UK.
[3]Dept. Atmospheric Sciences, University of Washington, Seattle, Washngton, USA.
[4]Science Systems and Applications, Inc., Lanham, Maryland, USA.
[5]Bay Area Environmental Research Institute, Sonoma, California, USA.

Copyright 2003 by the American Geophysical Union.
0094-8276/03/2003GL017068$05.00

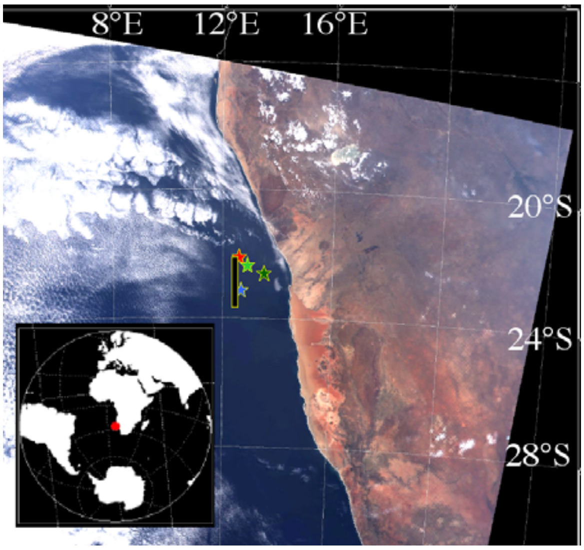

Figure 1. MODIS image of the area of the investigation from Sept. 11, 2000. The black line is the path of the ER-2 aircraft with the lidar aboard. The green, blue and red stars show the area of operation of the C-130 and the CV-580 aircraft, corresponding to the data in Figures 3 and 4.

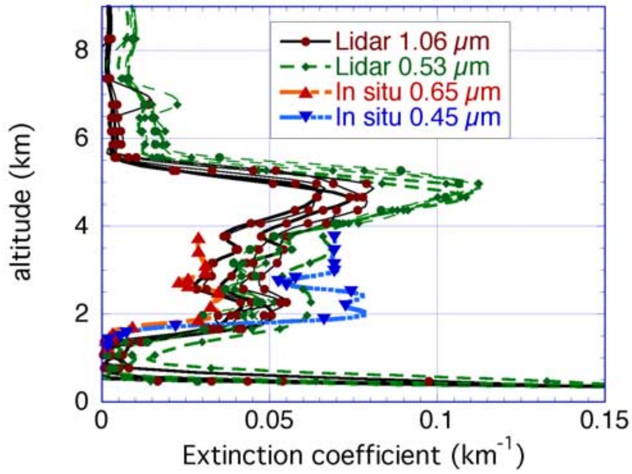

Figure 3. Extinction coefficient at 0.53 (green lines) and 1.06 μm (black lines) inverted from the 5 lidar profiles and MODIS spectral measurements. In situ measurements from the CV-580 of the scattering coefficient, converted to extinction are shown in red and blue for the 0.65 μm (ω_o = 0.87) and 0.45 μm (ω_o = 0.91), respectively. The MODIS and lidar data were collected at 0930–1000 UTC and the in situ measurements at 1030–1100 UTC, Sept. 11, 2000.

Figure 3 and compared with the inversion of the lidar and MODIS data.

3. Inversion of the Lidar and Modis Data

[7] The detailed inversion procedure is given by *Kaufman et al.* [2003], a short summary follows. The inversion is performed in two steps: (1) inversion of the lidar data alone 20 times, each for a different combination of one out of four predetermined fine aerosol models and one out of five coarse aerosol models (see Table 1). Two spectral channels are used to derive profiles of the extinction coefficient, σ_e, and fraction of the fine mode aerosol, η_f. Since for each of the 20 combinations the properties of the fine and coarse modes are predetermined, and assumed not to vary with altitude, the inversion is straight forward [*Kaufman et al.*, 2003]. It starts from the top aerosol layer, correcting the attenuated back-scattering coefficients for scattering above the given layer. The value of η_f is derived from the spectral ratio of the measured backscattering coefficients at 0.53 μm (β_{m5}) and 1.06 μm (β_{m1}) corrected for attenuation:

$$\xi_m = \beta_{m1}/\beta_{m5} \qquad (1)$$

The ratio β_{m1}/β_{m5} can be expressed by the ratio of the backscattering to extinction ratios: b_{5f}, b_{5C} b_{1f} and b_{1C} for each mode at 0.53 and 1.06 μm respectively. Therefore, for a layer at altitude z:

$$\xi_m(z) = [\eta_f(z)b_{1f} + (1-\eta_f(z))b_{1C}]/[\eta_f(z)b_{5f} + (1-\eta_f(z))b_{5C}] \qquad (2)$$

$$\eta_f(z) = [b_{1c} - \xi_m(z)b_{5c}]/[\xi_m(z)b_{5f} - \xi_m(z)b_{5c} - b_{1f} + b_{1c}] \qquad (3)$$

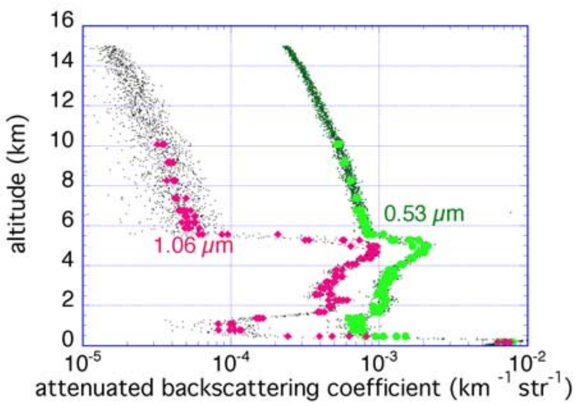

Figure 2. Five profiles of the lidar backscattering coefficients at 0.53 μm and 1.06 μm. Small dots 15 m vertical resolution, large symbols averaged on 300 m layers below 7 km altitude and 900 m layers above. The lidar was calibrated against molecular scattering in the upper part of the atmosphere. The signal to noise ratio at 1.06 μm is 16 times smaller than at 0.53 μm and the quantum efficiency is ~10 times lower resulting in higher calibration uncertainty.

Table 1. Aerosol Models for the Fine and Coarse Aerosols Used in the Inversion

Fine aerosol			Coarse aerosol		
R_{eff} μm	BER (sr^{-1}) 0.53 μm	Description	R_{eff} μm	BER (sr^{-1}) 0.53 μm	Description
0.10	0.022	Dry	1.0	0.035	Sea salt
0.15	0.016	Intermediate	1.5	0.035	Sea salt
0.20	0.013	Wet	2.0	0.032	Sea salt
0.25	0.013	Wet large	1.5	0.076	Dust
			2.0	0.073	Dust

R_{eff} is the effective aerosol particle radius and BER = $\omega_o P(180)/(4\pi)$ is the backscattering-to-extinction ratio for spherical Mie particles. The single scattering albedo was taken as $\omega_o^{0.53} = 0.90$ and $\omega_o^{1.06} = 0.85$ – [*Haywood et al.*, 2003] and extrapolated linearly for other MODIS wavelengths.

The extinction profile is derived from:

$$\sigma_{e5}(z) = b_{m5}(z)/[b_{5f}\eta_f(z) + \{1 - \eta_f(z)\}b_{5c}] \quad (4)$$

[8] The inversion derives two aerosol parameters, namely, the extinction coefficient and fraction of fine mode aerosol from the two lidar measurements. In other words, for a given combination of a fine and a coarse aerosol model, a unique profile of the optical thickness of the fine and coarse aerosols is derived from the lidar data. However, only one of the 20 combinations can be correct. MODIS data are used to select the best fitting combination. For each of the 20 profiles the spectral reflectance measured by MODIS is computed and compared with the measured one. The combination that gives the best fit is selected as the actual profile.

4. Results

[9] Inversion of the lidar attenuated backscattering coefficients (Figure 2) with the MODIS spectral radiances provides profiles of the extinction coefficient, $\sigma_{e5}(z)$ and the fraction of fine aerosols, $\eta_f(z)$. It also identifies the fine and coarse models: f and C. The error in the fit of the MODIS spectral radiances is an indicator for the appropriateness of the aerosol model. We found that the original BER values, given in Table 1, combined with the lidar calibration gave errors of 15–20% in fitting the MODIS spectral radiances. To reduce the error, we allow for an adjustment in the BER values of the coarse mode and adjustments in the lidar calibration from one case to another. Table 2 summarizes the results for the five analyzed cases. The BER values of the coarse aerosol was adjusted to 60% and 40% of their values for the 0.53 and 1.06 μm channels, respectively. This is in general agreement with the finding of *Haywood et al.* [2003] that the coarse mode of the smoke is non-spherical. The single scattering albedo, ω_o, and phase function of the fine aerosol was adjusted for the higher absorption of smoke aerosol ($\omega_o^{0.53}$ = 0.90 and $\omega_o^{1.06}$ = 0.85 – *Haywood et al.* [2003]). The resultant BER values are (0.017, 0.021 sr^{-1}) for the fine aerosol and (0.020, 0.014 sr^{-1}) for the coarse aerosol, at (0.53, 1.06 μm) respectively, which are similar to the value of 0.016 sr^{-1} reported for dust at both wavelengths by *Kaufman et al.* [2003]. *Mishchenko et al.* [1997] showed that the value of the spheroids phase function in the back scattering direction is half of the values for spheres for radius of 2 μm, making it closer to the value of the phase function for fine aerosols. For comparison, the BER values computed from Table 2 of *McGill et al.* [2003] are 0.014–0.024 sr^{-1} at 0.53 μm and 0.028–0.031 sr^{-1} at 1.06 μm.

Table 2. Results of the Inversion of the Lidar and MODIS Data. AOT is the Optical Thickness of the Aerosol Layer

Case	A	B	C	D	E	Average
AOT 0.53 μm	0.43	0.44	0.45	0.42	0.41	0.43 ± 0.02
AOT 1.06 μm	0.30	0.31	0.32	0.36	0.36	0.33 ± 0.03
Fraction of fine aerosol	0.45	0.48	0.48	0.33	0.31	0.41 ± 0.08
Error in MODIS fit %	2.9	2.7	2.6	2.0	1.6	2.4
R_{eff}-fine μm	0.15	0.15	0.15	0.20	0.15	0.16 ± 0.02
R_{eff}-coarse μm	2.0	2.0	2.0	1.5	1.5	1.8
Lidar calibration 0.53	1.03	0.99	0.97	0.99	1.01	1.00 ± 0.02
Lidar calibration 1.06	1.18	0.97	0.98	1.05	1.00	1.04 ± 0.09
NS coarse 0.53 μm	0.60	0.60	0.60	0.60	0.60	0.60
NS coarse 1.06 μm	0.40	0.40	0.40	0.40	0.40	0.40

NS is the non-sphericity reduction in the backscattering-to-extinction ratio.

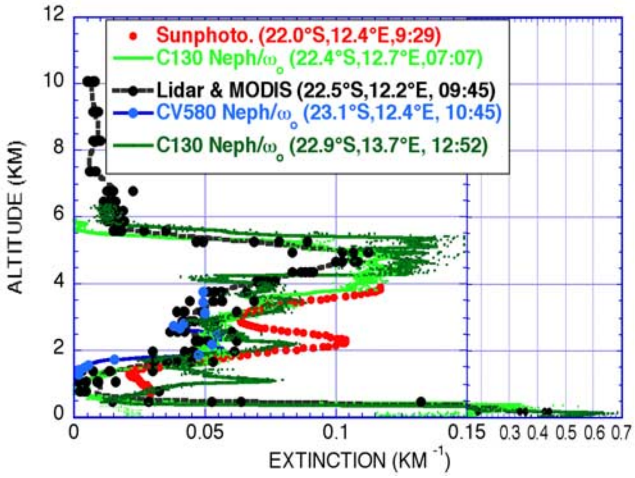

Figure 4. Extinction profiles derived from the lidar & MODIS data (black), in situ nephelometer measurements from the CV-580 (blue) and the C-130 (light and dark green) corrected for aerosol absorption using $\omega_o^{0.53}$ = 0.90, and for the difference between the ambient and the nephelometer relative humidity within the boundary layer assuming that the aerosol is sea-salt [*Ten Brink et al.*, 2000]. The AATS-14 sunphotometer measured extinction profile (red) for wavelength of 0.55 μm.

[10] The remote sensing results are compared with profiles of extinction coefficient measured in situ (Figures 3 and 4). Profiles of the scattering coefficient were measured from the CV-580 and C-130 aircraft, converted to extinction using the spectral single scattering albedo. An extinction profile was also derived from measurements of aerosol optical thickness by the Ames Airborne Tracking 14-channel Sunphotometer aboard the CV-580 aircraft [*Schmid et al.*, 2003]. The in situ measurements clearly show the presence of the smoke layer between 2 and 5 km, and a boundary layer humid aerosol in the lowest 600 m, similar to the lidar and MODIS inversion (Figure 4). The geometric thickness of the smoke layer varies with time, with a better fit to the inverted data of in situ measurements at 12:52.

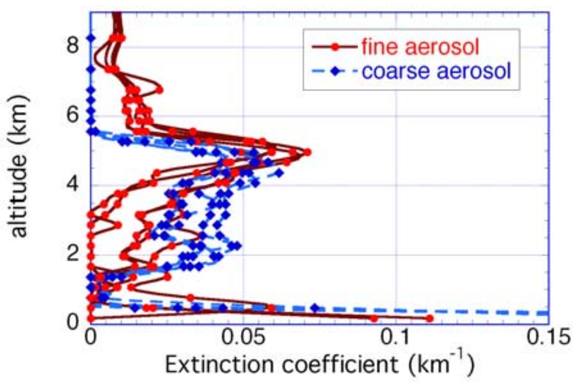

Figure 5. Profiles of the extinction coefficients of the fine (black) and coarse (gray) aerosol derived from the inversion of the lidar and MODIS data.

Table 3. Sensitivity of the Inversion to Changes in the Calibration (Case A and B Relative to O) and Nonsphericity (Case C Relative to O) of the Aerosol

Parameter \ Case	O	A	B	C
AOT: 0.53, 1.06 μm	0.44, 0.30	0.68, 0.31	0.63, 0.35	0.75, 0.30
Fraction fine aerosol	0.50	0.51	0.74	0.87
Error in MODIS fit %	3.3	9	11	27
Fine mode R_{eff}	0.15 μm	0.25 μm	0.25 μm	0.20 μm
Coarse mode R_{eff}	2.0 μm	2.0 μm	2.0 μm	1.5 μm
lidar calibration factor 0.53μm, 1.06 μm	1.04, 1.18	1.00, 1.15	1.00, 1.00	1.04, 1.18
Nonsphericity factor - coarse 0.53, 1.06 μm	0.60, 0.40	0.60, 0.40	0.60, 0.40	1.00, 1.00

[11] The optical thickness of the smoke layer at 0.55 μm is 0.35 and 0.39 from the C-130 two profiles and 0.31 ± 0.02 for the inverted data sets. The boundary layer (altitude < 0.6 km) has optical thickness of 0.11 ± 0.01 according to the inverted data and 0.10 to 0.13 according to the C-130 measurements for the humidified aerosol. The profile of the smoke layer (2–6 km) derived from the MODIS & lidar data at 9:45, fits better the later in situ data than the earlier sunphotometer and in situ data. Note that the spectral dependence of the aerosol in the 0.45–0.65 μm range measured by the nephelometers is larger than that of the inverted data in the 0.53–1.06 μm spectral range. The Ångström exponent computed for the smoke layer is around 2.0 for the in situ and sunphotometer measurements from the aircraft but only 0.74 for the lidar inverted data.

[12] The size distribution of the column aerosol derived in the inversion of MODIS and lidar data is composed of fine aerosol with effective radius of 0.16 ± 0.02 μm and coarse aerosol, identified as salt with effective radius of 1.8 ± 0.2 μm. These values are similar to the maxima of the volume distributions given by [*Haywood et al.*, 2003].

[13] Profiles of the extinction coefficient, $\sigma_{e5}(z)$, and the fraction of fine aerosol, $\eta_f(z)$, are converted to independent profiles of the fine $\sigma_{5f}(z)$ and coarse $\sigma_{5C}(z)$ aerosol extinction at 0.53 μm:

$$\sigma_{5f}(z) = \sigma_{e5}(z)\eta_f(z); \sigma_{5C}(z) = \sigma_{e5}(z)[1 - \eta_f(z)] \quad (5)$$

[14] Results are shown in Figure 5. The profile of the coarse aerosol is shifted down in altitude, as expected due to gravitational settling of the heavier coarse aerosol, or due to a different origin of the aerosol above 4 km.

5. Discussion

[15] The inversion of active and passive remote sensing data of aerosol was found to agree well with in situ measured profiles of the extinction coefficient, but resulted in a smaller wavelength dependence than measured. This is a typical problem with MODIS, unrelated to the MODIS-lidar retrievals. MODIS derives correctly the aerosol effective radius but underestimates the Ångström exponent for fine aerosol [*Remer et al.*, 2002]. In the inversion, the BER values of the coarse aerosol and the lidar calibration had to be adjusted. This can be a source of instability in global applications. Table 3 summarizes the sensitivity of the inversion to these parameters. Note that the MODIS calibration accuracy, and the wide spread of the model parameters in Table 1, calls for a fit with an error of <3% to the MODIS data in most cases [*Tanré et al.*, 1997]. However, the large errors of 9–27% obtained without adjusting either the lidar calibration or the aerosol nonsphericity, is excessively large. Lidar calibration is performed by recording the lidar return from high aerosol-free layers. However, noise in the data, especially at 1.06 μm, can result in errors in calibration for these low signals. Therefore, it is recommended that for significant aerosol concentration (e.g., optical thickness >0.2), the lidar calibration be adjusted to minimize the error in fitting the MODIS data.

References

Anderson, T. L., and J. A. Ogren, Determining aerosol radiative properties using the TSI 3563 integrating nephelometer, *Aerosol Sci. and Technol.*, *29*, 57–69, 1998.

Haywood, J. M., and O. Boucher, Estimates of the direct and indirect radiative forcing due to tropospheric aerosols: A review, *Revs. Geophys.*, *38*, 513–543, 2000.

Haywood, J. M., et al., The mean physical and optical properties of regional haze dominated by biomass burning aerosol measured from the C-130 aircraft during SAFARI 2000, *J. Geophys. Res*, *108*(D13), 8473, doi:10.1029/2002JD002226, 2003.

Hobbs, P. V., Technical Appendix: An overview of the Univ. of Washington's airborne measurements in the SAFARI 2000 field study in southern Africa, *J. Geophys. Res.*, *108*(D13), 8485, 2003.

Kaufman, Y. J., D. Tanré, and O. Boucher, A satellite view of aerosols in the climate system, *Nature*, *419*, 215–223, Review for, 2002.

Kaufman, Y. J., D. Tanré, J.-F. Léon, and J. Pelon, Retrievals of profiles of fine and coarse aerosols using lidar and radiometric space measurements, Accepted to IEEE: TGRS, 2003.

Lelieveld, J., et al., Global air pollution crossroads over the Mediterranean, *Science*, *298*, 794–799, 2002.

Léon, J. F., et al., Profiling of a Saharan dust outbreak based on a synergy between active and passive remote sensing synergy, *J. Geophys. Res*, accepted for, 2003.

McGill, M. J., Airborne lidar measurements of aerosol optical properties during SAFARI-2000, *J. Geophys. Res.*, *108*(D13), 8493, doi:10.1029/2002JD002370, 2003.

Menon, S., J. Hansen, L. Nazarenko, and Y. Luo, Climate effects of black carbon aerosols in China and India, *Science*, *297*, 2250–2253, 2002.

Mishchenko, M. I., et al., Modeling phase functions for dustlike tropospheric aerosols using a shape mixture of randomly oriented polydisperse spheroids J, *Geophys. Res.*, *102*, 16,831–16,847, 1997.

Ramanathan, V., P. J. Crutzen, J. T. Kiehl, and D. Rosenfeld, Atmosphere—Aerosols, climate, and the hydrological cycle, *Science*, *294*, 2119–2124, 2001.

Remer, L. A., et al., Validation of MODIS aerosol retrieval over ocean, *Geophys. Res. Lett.*, *29*(12), 1618, 2002.

Schmid, B., et al., Coordinated airborne, spaceborne, and ground based measurements of massive, thick aerosol layers during the dry season in southern Africa, *J. Geophys. Res.*, *108*(D13), 8496, doi:10.1029/2002JD002297, 2003.

Spinhirne, J. D., R. Boers, and W. D. Hart, Cloud Top Liquid Water from Lidar Observations of Marine Stratocumulus, *J. Clim. Appl. Meteorol.*, *28*, 81, 1989.

Swap, R. J., et al., The Southern African Regional Science Initiative (SAFARI 2000): Overview of the dry season field campaign, *S. African J. Sci.*, *98*, 125–130, 2002.

Tanré, D., Y. J. Kaufman, M. Herman, and S. Mattoo, Remote sensing of aerosol over oceans from EOS-MODIS, *J. Geophys. Res*, *102*, 16,971–16,988, 1997.

Ten Brink, H. M., et al., A high-flow humidograph for testing the water uptake of ambient aerosol, *Atmos Env.*, *34*, 4291–4300, 2000.

Y. J. Kaufman, NASA Goddard Space Flight Center, Laboratory for Atmospheres, Greenbelt, MD 20771, USA. (kaufman@climate.gsfc.nasa.gov)

J. M. Haywood, Met Office, Bracknell, UK.

P. V. Hobbs, Dept. Atmospheric Sciences, University of Washington, Box 351640, Seattle, WA 98195-1640, USA.

W. Hart and R. Kleidman, Science Systems and Applications, Inc., Lanham, MD 20706, USA.

B. Schmid, Bay Area Environmental Research Institute, Sonoma, CA 95476, USA.